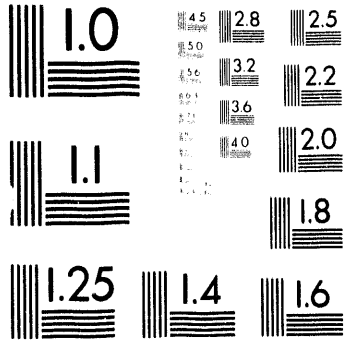
1.0
1.1
1.25
1.4
1.6
1.8
2.0
2.2
2.5
2.8
3.2
3.6
4.0
4.5
5.0
5.6

1 of 1

CONF-9309228--2

LA-UR- 93-3299

Title: Effects of Magmatic Activity on the Potential Yucca Mountain Repository: Field and Computational Studies

Author(s): G.A. Valentine
K.R. Groves
C.W. Gable
F.V. Perry
B.M. Crowe

Submitted to: Proceedings, Focus 93
Las Vegas, 27-29 September 1993

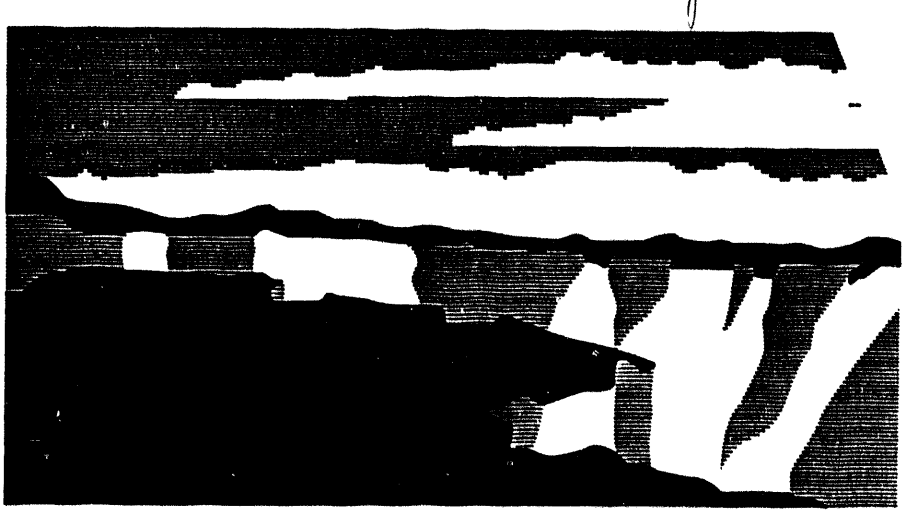

Los Alamos
NATIONAL LABORATORY

Form No. 836 R5
ST 2629 10/91

EFFECTS OF MAGMATIC PROCESSES ON THE POTENTIAL YUCCA MOUNTAIN REPOSITORY: FIELD AND COMPUTATIONAL STUDIES

G.A. Valentine, K.R. Groves, & C.W. Gable
Geoanalysis Group EES-5
Mail Stop F665
Los Alamos National Laboratory
Los Alamos, NM 87545

F.V. Perry & B.M. Crowe
Nuclear Waste Management
Research & Development
Group EES-13, MS J521
Los Alamos National Laboratory
Los Alamos, NM 87545

ABSTRACT

Assessing the risk of future magmatic activity at a potential Yucca Mountain radioactive waste repository requires, in addition to event probabilities, some knowledge of the consequences of such activity. Magmatic consequences are divided into an eruptive component, which pertains to the possibility of radioactive waste being erupted onto the surface of Yucca Mountain, and a subsurface component, which occurs whether there is an accompanying eruption or not. The subsurface component pertains to a suite of processes such as hydrothermal activity, changes in country rock properties, and long term alteration of the hydrologic flow field which change the waste isolation system. This paper is the second in a series describing progress on studies of the effects of magmatic activity. We describe initial results of field analog studies at small volume basaltic centers where detailed measurements are being conducted of the amount of wall rock debris that can be erupted as a function of depth in the volcanic plumbing system. Constraints from field evidence of wall rock entrainment mechanisms are also discussed. Evidence is described for a mechanism of producing subhorizontal sills versus subvertical dikes, an issue that is important for assessing subsurface effects. Finally, new modeling techniques,

which are being developed in order to capture the three dimensional complexities of real geologic situations in subsurface effects, are described.

INTRODUCTION

The risk of future magmatic activity for the potential Yucca Mountain repository block is defined by the conditional probability

$$Pr_{dr} = Pr(E3 \text{ given } E2,E1)Pr(E2 \text{ given } E1)Pr(E1) \quad ,$$

where Pr_{dr} is the magmatic disruption probability (i.e., the likelihood of a magmatic event causing release of radioactive waste to the accessible environment in excess of regulatory limits), *E1* is the recurrence rate of magmatic events in the Yucca Mountain region, *E2* is the probability that a future magmatic event intersects the repository or is close enough to have a significant effect on repository performance, and *E3* is the probability that a given magmatic event will cause release of waste to the accessible environment in quantities that exceed regulatory limits. *E3* is the sum of two components, $E3_e$ and $E3_s$, which denote release to the surface by eruption and release in the subsurface environment, respectively. Pr_{dr} is the primary measure for judging reduction in waste isolation as a result of magmatic processes. Research associated with E3 is divided into three parts:[1] (1) Eruptive Effects ($E3_e$), which addresses how much radioactive waste could be erupted onto the surface of Yucca Mountain if an eruptive event penetrated the potential repository; (2) Subsurface Effects ($E3_s$), which addresses processes such as local hydrothermal circulation or perturbation of the regional groundwater flow field in response to an intrusive event (with or without eruption); (3) Magma System Dynamics, which addresses, from a physical point of view, the overall processes that produce the

observed patterns of volcanism in the Yucca Mountain region with the goal of supporting the conceptual basis for event probability calculations.

This paper is a sequel to the 1992 paper of Valentine et al.,[2] which was the first published report describing recent efforts to understand and estimate the effects of magmatic activity on the potential Yucca Mountain repository. This earlier paper[2] focused on strategies that had been identified for estimating eruptive and subsurface effects, and described initial studies of subsurface effects at the Paiute Ridge analog area, along with initial efforts at modeling magma system dynamics. Since that paper was written, work has proceeded on both eruptive effects and subsurface effects, and to a lesser extent general concepts of magma dynamics. The current paper will emphasize initial results of eruptive effects studies.

ERUPTIVE EFFECTS ($E3_e$) STUDIES

Xenolith Abundances at Small Basaltic Centers

Valentine et al.[1,2] have described the importance of using analog basaltic centers to constrain the amount of foreign material that could be erupted onto the Earth's surface from a given depth, which in our case is the depth of the potential repository horizon. Analog studies are more desirable than theoretical studies because the physics of wall rock entrainment into magma flowing through a dike is only poorly known. Our approach is to identify basaltic centers of similar size, composition, and eruptive styles to the Pliocene-Quaternary centers near Yucca Mountain. The additional factor is added that the sub volcanic rock types are well known and their depths beneath the volcanoes are well constrained. We then conduct detailed measurements of crustal xenolith abundances and attempt to correlate each xenolith with its depth of origin (if possible). These data then

provide quantitative information on the amount of debris, including radioactive waste, which could be erupted from the potential repository horizon. There are limited studies in the literature that describe the volume fraction of shallow crustal xenoliths (*a.k.a.* lithics) in small volume Strombolian and hydrovolcanic volcanoes such as those near Yucca Mountain,[3-5] but these generally do not contain detailed data on the relative proportions and depths of derivation of the lithics. The only paper that we are familiar with that provides data on proportions of lithics as functions of depth of origin is that of Mastin,[6] which is about a rhyolite dome, not a basaltic center.

The Colorado Plateau provides an excellent setting for this study because of its well established, subhorizontal stratigraphy that is relatively unaffected by faulting; our initial work has been conducted on the eastern margin of the Colorado Plateau in the Lucero volcanic field, west-central New Mexico.[7] Basaltic volcanism in the Lucero field ranges in age from 8.3 Ma to as recent as a few thousands or tens of thousands of years. Eruptive styles ranged from broad shields with lava flows extending several tens of kilometers, to small isolated scoria cones, tuff rings, and tuff cones. Compositions are mainly tholeiite to alkali basalts.

To date we have focused on the Alkali Buttes centers (Figure 1; see also Ref. 7), which are thought to be several hundred thousand years old. These buttes are erosional remnants of an approximately 2 km long, north-northeast trending, chain of four to five vents that is subparallel to major normal faults in the area. This chain probably formed a single continuous land form prior to erosion. South Alkali Butte is the remnant of a tuff ring or tuff cone (only the crater-filling deposits are preserved). The earliest deposits are lapilli tuffs containing abundant lapilli and block-sized lithic clasts, probably representing strongly hydrovolcanic activity. These tuffs are overlain by relatively ash poor beds of poorly vesicular basalt lapilli with much lower lithic content than the tuffs. These lapilli

beds probably represent eruptions that were influenced by a lower degree of hydrovolcanic fragmentation than the underlying tuffs. Overlying the lapilli beds are beds of coarse, vesicular scoria and small bombs, which are in turn overlain by variably agglutinated coarse spatter beds interlayered with thin lava and pillow lava flow units. Near the original crater center, the spatter beds are overlain by a mixture of mud derived from the Chinle formation (see below) and large, highly vesicular fluidal basalt clasts. The entire sequence is capped by pillow lavas which locally protrude downward into the Chinle-basalt mixture. We interpret this sequence as recording decreasing hydrovolcanic activity through the main phases of eruption (lapilli tuffs, poorly vesicular lapilli, scoria, and spatter/lava flow units). This phase was followed by an extended period of weak lava effusion and mud boiling in the lowest parts of the crater (to produce the mixed Chinle mud-basalt clast unit) and eventually production of a small volume of lava which flowed onto and into the mixed Chinle mud-basalt clast unit. The latter unit was probably a water-saturated slurry at the time (hence the formation of pillow lavas). A small area, about 50 m in diameter, on the interior of the center is littered with large (decimeter to meter) sized lithic blocks from 500-600 m depth, perhaps indicating a late-stage phreatic explosion. Possible hot spring deposits capping pillow lava in the center of the original crater indicate that hydrothermal activity persisted for some time after eruptions ceased.

North Alkali Butte consists of the remnants of three scoria/spatter cones and associated craters (Figure 1). The southern two cones filled in a previously formed tuff ring or tuff cone, of which only the inner, inward dipping deposits are preserved. As at South Alkali Butte, the lowest preserved deposits of this tuff ring/cone phase are lapilli tuffs, overlain by poorly vesicular basalt lapilli beds, then vesicular scoria and spatter beds that are variably agglutinated and are associated with the three cones. Localized lava flows were also erupted from the cones but, unlike South Alkali Butte, we found no pillow lavas. This is probably because the cones filled up the tuff ring/cone's crater to produce

topographic highs. This contrasts with South Alkali Butte where the crater was not filled and thus remained a closed basin which retained water and the Chinle/lava slurry described above. The northern part of North Alkali Butte is poorly exposed, but does not seem to contain the hydrovolcanic units (lapilli tuffs and poorly vesicular lapilli beds) that occur to the south. Additionally, it may not have experienced extensive hydrovolcanic processes. Possible hot spring deposits occur on the northeast flank of North Alkali Butte. An active spring is present at the southern end of North Alkali Butte; it is collinear with the possible hot spring deposits on North and South Alkali Buttes, along a north-northeasterly trend that like the trend of the vents is subparallel to regional normal faults. North Alkali Butte was more dominated by Strombolian eruption mechanisms (driven by expansion of magmatic volatiles) than South Alkali Butte, which had a larger hydrovolcanic component.

The sub volcanic stratigraphy at Alkali Buttes is well constrained due to exposure in the nearby Lucero Uplift[8,9] and two exploratory oil wells provide subsurface control. One of these wells is located about 22 km southwest of Alkali Buttes[10] and the other is located 14 km to the northwest of Alkali Buttes.[11] Strip logs for these wells were obtained at the New Mexico Bureau of Mines and Mineral Resources in Socorro, New Mexico. The stratigraphic units consist of, in descending order:

Chinle Formation (Upper Triassic) -- Approximately 510 m thick. Mainly red to reddish brown and purple silty mudstone and clay shale with thin sandstone lenses. Lower 200 m has zones of feldspathic sandstone, and chert and limestone pebble conglomerates.

San Andres Formation (Lower Permian) -- Approximately 130 m thick. Mainly gray fine to medium grained limestones, silty limestones, gypsum, and gypsiferous shale. Distinctive petroleum odor when broken.

Glorieta Sandstone (Lower Permian) -- Approximately 60 m thick. Massive, pale yellow, fine-grained, well-sorted quatzose sandstone with abundant cross bedding. Erosionally resistant formation.

Yeso Formation (Lower Permian) -- Approximately 400 m thick. Alternating beds of pale red, yellow, and buff gypsiferous shale with grayish white to pink sandstone. Highly gypsiferous.

Abo Formation (Lower Permian) -- Approximately 280 m thick. Mainly dark red, silty sandstones and shales with lenses of limestone.

Madera Formation (Pennsylvanian) -- Approximately 230 m thick. Various combinations of tan, gray, white, and red dense limestone interbedded with white, coarse-grained sandstone and light gray to red-brown shale.

Sandia Formation (Pennsylvanian) -- Approximately 75 m thick. Tan-white and tan-brown, dense, crystalline limestone interbedded with white coarse-grained sandstone and conglomerate.

Granite Wash Formation (Precambrian) -- Coarsely crystalline granite.

The approximate thicknesses given above are estimated to be accurate to within 10% of the thickness of each formation. Most observed lithic fragments were from the Chinle, San Andres, or Glorieta formations (depths less than about 700 m).

Preliminary lithic abundance data for the Alkali Buttes centers are shown in Figures 2, 3. We have grouped the data according to the eruption facies to which they correspond, instead of specific stratigraphic or geographic locations, because our main interest here is the influence of different eruptive mechanisms on lithic abundances. Note that many more basaltic centers will be studied in order to minimize the effects of local geologic conditions on our results, which will ultimately be applied to the Yucca Mountain setting. Lithic abundance data were collected by marking off 1 m^2 with nails and a string, then measuring the long and short dimension of each lithic fragment within the area and identifying the formational origin. In some cases, especially for smaller clasts or clasts that had been baked (for example, a lithic clast within a lava bomb), the identifications were ambiguous. For the plots shown we lumped these clasts, which are a minor part of the data, with their most likely formations. Only clasts with a long dimension of 1 cm or greater were measured in the field; the abundance of smaller lithic clasts will be determined from microscopic examination of samples collected within the measured areas. Thus the data shown here are only the macroscopic component of lithics. When microscope data are included the total abundances will increase somewhat, particularly in the lapilli tuffs where it is likely that much of the ash matrix is xenolithic. Using the long and short dimension of each measured clast, we compute the area of the clast in the outcrop by approximating it as a rectangle. These areas are converted to area fractions by tallying the areas of all lithics of a given formation. The area fraction is proportional to volume fraction, although some correction will eventually be made for the fact that not all lithics are exposed at their maximum cross sectional area. This correction will probably result in a 30-40% increase in converting area fractions to volume fractions.

Overall, we feel that that the error in the area fraction estimates is about 10%. A more rigorous assessment of th s error will be made in the future.

Figure 2 shows lithic abundances (area fractions) as functions of depth for lapilli tuffs, poorly vesicular lapilli units, and vesicular scoria/spatter units. Also shown are total lithic abundances for each measured area. Note that we have plotted depths for each lithic type at mid level for each particular formation; each point should be considered as having a possible depth range over the entire thickness of that formation. Most of the plots show a general decrease in lithic abundance with increasing depth of origin. This simple trend is complicated by the fact that Glorieta Sandstone fragments are typically more common than fragments from the overlying San Andres Formation. There are at least two possible reasons for this. First, although the Glorieta Sandstone is very dense and has a low matrix porosity, it is highly fractured. It may therefore have acted as a fracture-dominated aquifer and therefore as a source of water for explosive magma-water interaction. The difference in abundance of fragments then reflects the relative importance of hydrovolcanic explosions at corresponding depths. This interpretation perhaps best applies for the lapilli tuffs and poorly vesicular lapilli units, which show independent evidence for an important role of hydrovolcanism (e.g., abundance of ash in the tuffs, low vesicularity of juvenile clasts). However, the vesicular scoria/spatter units, which seem to have been formed by eruptions driven mainly by magmatic volatiles, show the same trend in lithic abundances. A second and favored interpretation at this point is that the mechanical properties of the Glorieta Sandstone played the major role in controlling its abundance in eruptive deposits. In outcrop, Glorieta Sandstone is fractured into coherent blocks of various sizes that depend partly on the scale of bedding within the sandstones. This contrasts with the overlying San Andres and Chinle formations, which tend to be less competent and have a larger proportion of nonindurated shales and mudstones, with only thin layers of more competent limestones or sandstones. These formations may not

sustain fractures as well as the Glorieta Sandstone so that large coherent fragments do not break off as easily. Mechanisms for this entrainment will be discussed in the next section.

Figure 3 shows total area fraction of lithics and maximum lithic sizes for the main eruptive facies. Vertical bars within each facies type represent average values, which of course are based on only a few data at this point and are preliminary. The data show that in general the total lithic contents decrease upward in the stratigraphic sections (Figure 3a), paralleling the inferred decrease in importance of hydrovolcanic processes, which is expected. Maximum xenolith size, which is the average of the three largest lithic clasts measured at each station, also decreases between the lapilli tuffs and the vesicular spatter/scoria units. The largest lithic clasts measured in the lapilli tuffs to date are 2.2 m and 1.5 m in long dimension, and are from the San Andres and Glorieta Sandstone formations, respectively. Other lithic clasts of comparable size were, surprisingly, found in the vesicular spatter/scoria units at South Alkali Butte. These clasts are 2.7 and 3.0 m in long dimension, and are both from gypsum beds that are characteristic of the topmost Yeso Formation. Thus large meter-size blocks were erupted from depths of 500-700 m during both hydrovolcanic and magmatic eruptions at South Alkali Butte.

These are only preliminary data, but it is useful to describe briefly how they will be used to assess eruptive effects at the potential Yucca Mountain repository. Our approach is to collect such data at several sites in a variety of settings. For each eruptive mechanism (related to the deposit facies), we will compile a range of lithic abundances for depths corresponding to the depth of the potential repository horizon. The range of volume fractions from each eruptive mechanism will then be coupled with probabilities and likely eruptive volumes for the different mechanisms to estimate total volumes of repository horizon debris that could be erupted during a volcanic event. Assuming that radioactive waste behaves similarly to the surrounding rocks, we will directly estimate the

amount of actual waste erupted (we view this assumption as conservative for reasons detailed in Refs. 1, 2). Maximum xenolith size data provide constraints on the largest fragments that could be erupted in a repository disruption scenario.

Entrainment Mechanisms

It is important to understand the mechanisms by which foreign debris is entrained into a flowing dike or magma conduit in order to constrain the processes of waste disruption. As mentioned above, a theoretical treatment of this process has been elusive, so we have focused on evidence from analog sites. We have focused our initial studies on the Paiute Ridge[2,12,13] and Nye Canyon[14,15] analog sites, both of which are on the eastern border of the Nevada Test Site. Basalt intruded and erupted through silicic tuff from the Timber Mountain-Oasis Valley caldera complex at both sites, thus they are analogous to a potential basaltic event at Yucca Mountain where basalts would intrude similar tuffs. The Paiute Ridge and Nye Canyon sites have been eroded to depths of 100-300 m below their surfaces at the time of basaltic activity, so the processes recorded may be similar to those which would occur at repository depths in Yucca Mountain.

We have identified three main entrainment mechanisms at these analog sites (Figure 4): spalling of rock into the tip of a propagating dike, dike wall erosion due to shear from flowing magma, and inclusion of wall rock material between a main dike and small subparallel offshoot dikes. An additional mechanism, which we do not discuss in detail here, is explosive fracturing of wall rocks due to magma-water interaction. The first of these mechanisms, spalling into a dike tip, results from the very low pressures inside a crack that is just being pushed open[16] compared to the near lithostatic pressure in adjacent country rocks. Evidence for this process at Paiute Ridge consists of patches of brecciated wall rock along the margins of a dike (the dike is about 2 m thick) within 20 m of its upper

termination. This dike spays into two to three subparallel dikes near its termination, which probably aids in the entrainment process.

Dike wall erosion due to shear is physically similar to erosion of a stream bed. Asperities on a dike wall experience shear (and pressure variations) due to the flowing magma and if this shear is sufficiently strong the asperities will break off the walls. In competent rock such as well-cemented limestones and welded tuffs, this entrainment process is probably of minor importance. Less competent rocks, such as nonindurated shales and nonwelded tuffs, may be more strongly affected by this shear erosion process.

Inclusion of wall rocks between a main dike and subparallel offshoots is shown at a wide range of scales both at Paiute Ridge and at Nye Canyon. In one example at Paiute Ridge, a ~1 m thick main dike is separated by about 3 m from a thin (10-20 cm) offshoot dike. Between these two dikes the tuff wall rocks have been compressed and welded by the heat and pressure of the dikes in some places. In others the rocks have been extensively brecciated and form a complex mixture of wall rock breccia and injected basalt (some of the breccia may have been in existence prior to intrusion of the basalts due to a nearby normal fault). Patches of breccia extend into the main dike where they become mixed with progressively more basalt, indicating that the entrainment process was preserved in action when flow in the dike ceased. Numerous smaller scale examples of the inclusion mechanism are preserved at these two analog sites. Typically, small centimeter thick offshoot dikes will extend outward for several centimeters to a few tens of centimeters, then curve back inward to join the main dike. The small "islands" of wall rock are then caught up in the main flow of magma. We think that the abundance of xenoliths from the Glorieta Sandstone, mentioned in the preceding section, may be a result of this inclusion process. The fractured nature of the sandstone would enhance formation

of numerous offshoot dikes, which would result in incorporation of coherent blocks of sandstone more easily than in the overlying formations.

Of these mechanisms, the two that are most likely to effectively entrain intact or partially intact waste packages are the spalling of rock into a propagating dike tip and the inclusion of wall rocks between main dikes and offshoots. It is clear from the data at Alkali Buttes that blocks with dimensions that are similar to waste packages (1-2 m) can be erupted from depth in small basaltic eruptions, although these are relatively rare. If a volcanic event were to penetrate the repository late in the isolation period, after waste packages have corroded, it is likely that waste could be easily incorporated into a dike.

Conduit Geometries

A third aspect of our studies of eruptive effects, which also relates to subsurface effects, is conduit geometries for small basaltic volcanoes. Such volcanoes are fed at depth by dikes, but in the near surface environment these dikes flare and flow becomes concentrated into one or a few near cylindrical conduits. Such geometrical changes could influence the amount of waste that could be intersected by magma if a volcanic event occurred at the potential Yucca Mountain site. We are in the beginning stages of surveying deeply eroded centers where these features have been exposed. Many such plugs or necks are exposed in west central New Mexico where there are good constraints on the elevation of the ground surface at the time of eruptions. We are also studying such features in the southern Great Basin of Nevada, although it is often difficult to constrain original depths because of post volcanic faulting.

SUBSURFACE EFFECTS ($E3_S$) STUDIES

Dikes vs. Sills

The subsurface effects of a dike or dike set, which would be expected to be subvertical, are probably much different from the effects of a subhorizontal sill. These effects would be strongly influenced by the planform of hydrothermal circulation resulting from an intrusion and, in the long term, by intrusion-induced changes in hydrologic properties of the country rock. We must understand the mechanisms that cause sills to form at shallow depths (within 1 km of the surface) in order to place constraints on the probability of sill emplacement at Yucca Mountain. It is commonly assumed that sills form at a level of neutral buoyancy, where the magma and country rock densities are equal. Evidence from the Paiute Ridge analog site[2,13] suggests that other processes may be important in determining whether a sill is formed from a dike filled with rising magma. Here there are subvertical dikes several kilometers long, and typically only 1-3 m thick, from which sills extend horizontally only locally from the dikes. For example, a sill might extend horizontally from a 100 m long segment of the feeder dike that is several kilometers long. A single long dike can feed two or three separate sills along its length, all at roughly the same level (or depth below the original surface). In addition, at least two of the main feeder dikes extend 100 m or higher above the level of their daughter sills. These observations indicate that sills at Paiute Ridge result from a process other than a level of neutral buoyancy, which would cause a rising dike to divert into a sill along its entire length, and magma in the dike would not be able to flow above the level of neutral buoyancy. Most of the dikes at Paiute Ridge are coplanar with normal faults. We suggest that sills formed where asperities caused local locking along fault planes and hence local reorientation of principle stresses. We are currently exploring ways to test this hypothesis - unfortunately fault planes at Paiute Ridge are often obscured by coplanar intrusions and

poor exposure. If this hypothesis is true, then we will be able to utilize subsurface data on faults at Yucca Mountain to assess the probability of sill formation there, given an intrusive event.

Modeling

In addition to field analog studies of subsurface effects, we are using numerical simulation techniques to guide our understanding of the roles of various parameters (e.g., intrusion volume, country rock properties) on hydrothermal and long-term hydrologic processes. This modeling has three components: parameter sensitivity analysis under simplified conditions, simulation of processes at specific analog sites to improve our interpretations of observations, and simulations of subsurface effects at Yucca Mountain. These processes are inherently three dimensional and time dependent, and depend strongly on the distribution of country rock properties such as permeability and thermal conductivity. Therefore we have devoted most of our modeling effort in the past year to developing methods of capturing the complexities of real geologic settings.

A software package, MESHGEN, has been developed to build meshes for general problems, however, a three dimensional data base of Yucca Mountain stratigraphy produced by Sandia National Laboratory has been the main test data set (Figures 5, 6). The strategy of MESHGEN is to produce three dimensional tetrahedral meshes (or triangles in two dimensions) which follow the geometry of geologic formations. The use is able to specify variables such as: (1) horizontal and vertical resolution; (2) subsets of data to be extracted for detailed study (e.g., two dimensional cross sections or three dimensional blocks); minimum thickness of stratigraphic units to be represented in the computational mesh; and (4) unit conversion (e.g., input in feet, output in meters). The

final mesh produced is a Deleany mesh, which ensures that computations with the finite element code FEHMN will be accurate and stable.

We are currently using MESHGEN to generate meshes for flow and transport calculations for an area that completely encompasses the potential repository boundary. Once these calculations have been completed to establish baseline or ambient conditions, further calculations will investigate the influence of possible magmatic heat sources on the generation of hydrothermal flow in or near Yucca Mountain.

SUMMARY

We have briefly described recent progress in studies of eruptive and subsurface effects of magmatic activity, which will form part of the information that will be used for risk calculations and performance assessment. Eruptive effects studies to date have focused on analog studies of xenolith distribution at basaltic centers of the Lucero volcanic field, New Mexico, where well-characterized basement stratigraphy allows depths of origin to be assigned to erupted lithic fragments. Related field studies are constraining mechanisms by which waste might be entrained into a feeder dike in the event of a volcanic eruption at Yucca Mountain, as well as variations in the geometry of the volcanic plumbing with depth. Subsurface effects studies are focused on a variety of issues including the processes that produce sills, hydrothermal circulation, and long-term hydrologic processes. As these studies proceed, we believe that we will be able to place realistic constraints on the consequences of magmatism at the potential Yucca Mountain repository.

ACKNOWLEDGMENTS

This work is part of the U.S. Department of Energy's Yucca Mountain Site Characterization Project. Field data discussed above can be found in GAV's field notebooks TWS-EES-5-01-93-01 and TWS-EES-5-06-93-01. Computational work described herein has been carried out in a prototyping mode and has not been subject to software quality assurance measures.

REFERENCES

1. G.A. VALENTINE, B.M. CROWE, and F.V. PERRY, "Study Plan 8.3.1.8.1.2 Physical Processes of Magmatism and Effects on the Potential Repository," *YMP-LANL-SP-8.3.1.8.1.2*, Los Alamos National Laboratory (1993).

2. G.A. VALENTINE, B.M. CROWE, and F.V. PERRY, "Physical Processes and Effects of Magmatism in the Yucca Mountain Region," *Proceedings, 1992 Conference on High Level Radioactive Waste Management*, Las Vegas, pp. 2344-2355 (1992).

3. J.D.L. WHITE, "Maar-Diatreme Phreatomagmatism at Hopi Buttes, Navajo Nation (Arizona), USA," *Bulletin of Volcanology*, Vol. 53, pp. 239-258 (1991).

4. B.F. HOUGHTON and H.-U. SCHMINCKE, "Mixed Deposits of Simultaneous Strombolian and Phreatomagmatic Volcanism: Rothenberg Volcano, East Eifel Volcanic Field," *Journal of Volcanology and Geothermal Research*, Vol. 30, pp. 117-130 (1986).

5. B.F. HOUGHTON and H.-U. SCHMINCKE, "Rothenberg Scoria Cone, East Eifel: a Complex Strombolian and Phreatomagmatic Volcano," *Bulletin of Volcanology*, Vol. 52, pp. 28-48 (1989).

6. L.G. MASTIN, "The Roles of Magma and Groundwater in the Phreatic Eruptions at Inyo Craters, Long Valley Caldera, California," *Bulletin of Volcanology*, Vol. 53, pp. 579-596 (1991).

7. W.S. BALDRIDGE, F.V. PERRY, and M. SHAFIQULLAH, "Late Cenozoic Volcanism of the Southeastern Colorado Plateau: I. Volcanic Geology of the Lucero Area, New Mexico," *Geological Society of America Bulletin*, Vol. 99, pp. 463-470 (1987).

8. H.L. JICHA, Jr., "Geology and Mineral Resources of Mesa del Oro Quadrangle, Socorro and Valencia Counties, New Mexico," *Bulletin 56*, New Mexico Bureau of Mines and Mineral Resources (1958).

9. R.E. ZILINSKI, Jr., *Geology of the Central Part of the Lucero Uplift, Valencia County, New Mexico*, MS Thesis, University of New Mexico Geology Department (1976).

10 Spanel-Heinze oil well log, #1-M Santa Fe Pacific 9612, Log No. F-278, 5-5N-7W, total depth 4992 feet (1959).

11. E.R. HILL, Sun Oil Company oil well log, #1 Pueblo of Acoma, 2-7N-7W, total depth 4794 feet (1960).

12. F.M. BYERS, Jr., and H. BARNES, "Geologic Map of the Paiute Ridge Quadrangle, Nye and Lincoln Counties, Nevada," *Map GQ-577*, U.S. Geological Survey (1967).

13 B.M. CROWE, S. SELF, D. VANIMAN, R. AMOS, and F.V. PERRY, "Aspects of Potential Disruption of a High-Level Radioactive Waste Repository in Southern Nevada," *Journal of Geology*, Vol. 91, pp. 259-276 (1983).

14. E.N. HINRICHS and E.J. MCKAY, "Geologic Map of the Plutonium Valley Quadrangle, Nye and Lincoln Counties, Nevada," *Map GQ-384*, U.S. Geological Survey (1965).

15. B.M. CROWE, K.H. WOHLETZ, D.T. VANIMAN, E. GLADNEY, and N. BOWER, "Status of volcanic hazards studies for the Nevada Nuclear Waste Storage Investigations, Volume II," *LA-9325-MS*, Los Alamos National Laboratory (1986).

16. J.R. LISTER and R.C. KERR, "Fluid-Mechanical Models of Crack Propagation and Their Application to Magma Transport in Dykes," *Journal of Geophysical Research*, Vol. 96, pp. 10,049-10,077 (1991).

FIGURE CAPTIONS

Figure 1. Simplified geologic map of Alkali Buttes, showing distribution of volcanic rocks, dikes, inferred vents, inferred crater rims, possible hot spring deposits, and an active spring. Geographic location of Alkali Buttes can be found in Ref. 7. The volcanic rocks were erupted onto a surface cut into the Upper Triassic Chinle Formation.

Figure 2. Plots of macroscopic (> 1 cm long dimension) xenolith area fractions, measured on outcrops, against xenolith depth of origin. Sub volcanic stratigraphy is shown on the right hand side of each graph, corresponding to appropriate depths. (a) Lapilli tuff units,

(b) poorly vesicular lapilli units, and (c) vesicular spatter and scoria units. Value shown in a box by each curve is the total xenolith area fraction for that measured outcrop. Error bars are not shown, but a conservative estimate of error in area fraction values is +/-10% due to inaccuracies in measuring the outcrop area studied and because the area for each clast is computed as if the clast were a rectangle. Errors in the depth values are less constrained, and range over the entire thickness of each formation. Data have been plotted at mid level for each formation. For example, depth values for data plotted in the Chinle Formation have an error of +/-255 m. Data plotted at Glorieta Sandstone depths have errors of +/-30 m. Symbols. TRc - Chinle Formation; Ps - San Andres Formation; Pg - Glorieta Sandstone; Py - Yeso Formation; Pa - Abo Formation; Pm - Madera Formation.

Figure 3. Plots of total area fraction of xenoliths (a) and maximum xenolith size (b) for each of the four main volcanic facies at Alkali Buttes. Note that horizontal scales are logarithmic. Vertical bars represent average values for each facies type.

Figure 4. Mechanisms of wall rock entrainment into flowing dikes or conduits. (a) Wall rock spalls off into a propagating dike tip due to the low pressures there. (b) Entrainment by shear erosion of small fragments of wall rock. (c) Entrainment by inclusion, where small offshoot dikes separate fragments of wall rock which are then caught up in the flow of magma in the main dike.

Figure 5. Two dimensional triangular mesh used for finite element modeling of flow of transport at Yucca Mountain.

Figure 6. Representation of a three dimensional mesh used for modeling flow, transport, and hydrothermal processes at Yucca Mountain. The mesh has been expanded vertically to show how different stratigraphic units are represented. This is a finite difference mesh

(each computational cell is a rectangular brick) with a resolution of 75 m horizontally and 44 m vertically and has a total of 55,981 cells.

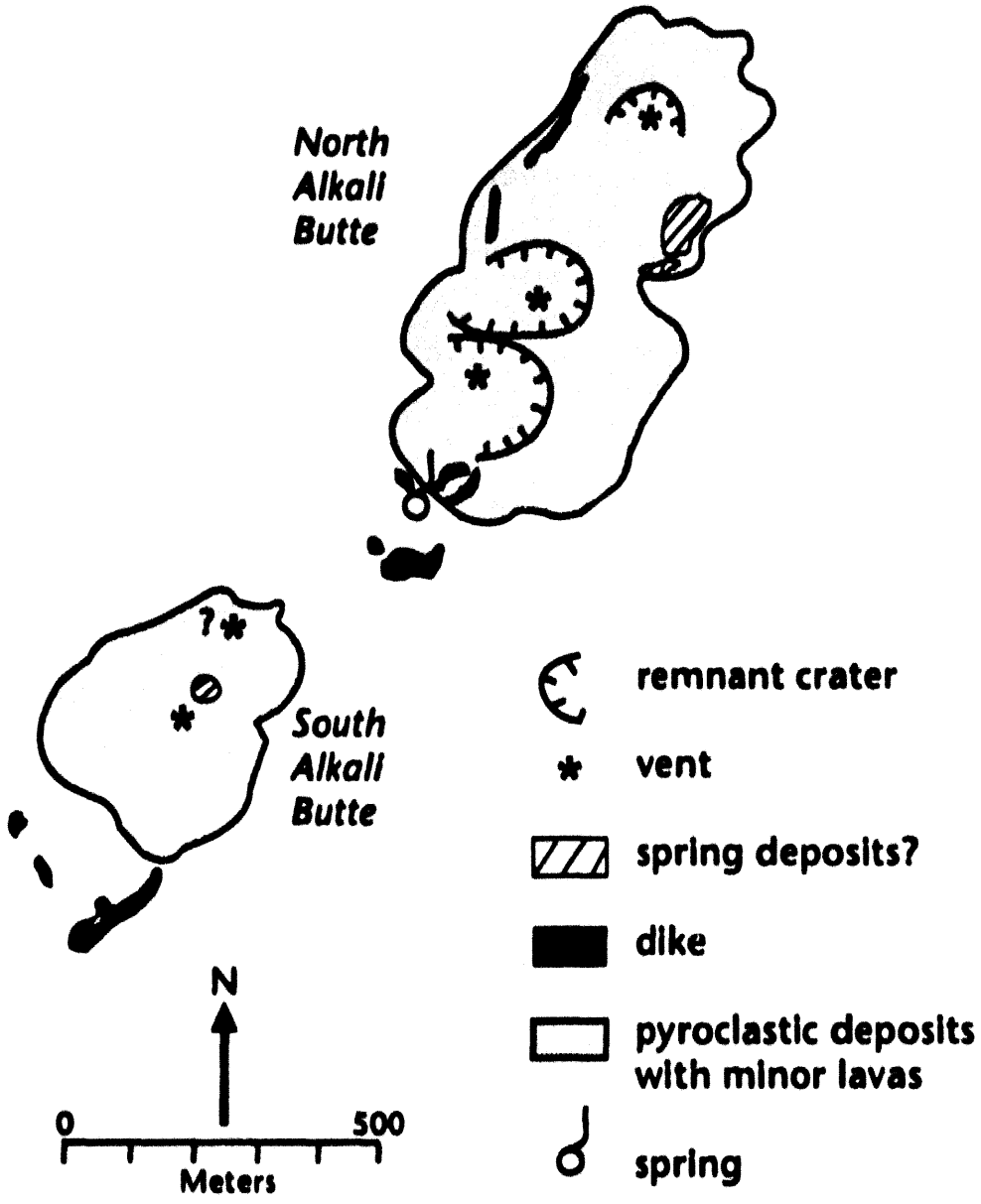
North
Alkali
Butte
South
Alkali
Butte
?
N
0
500
Meters
remnant crater
vent
spring deposits?
dike
pyroclastic deposits
with minor lavas
spring

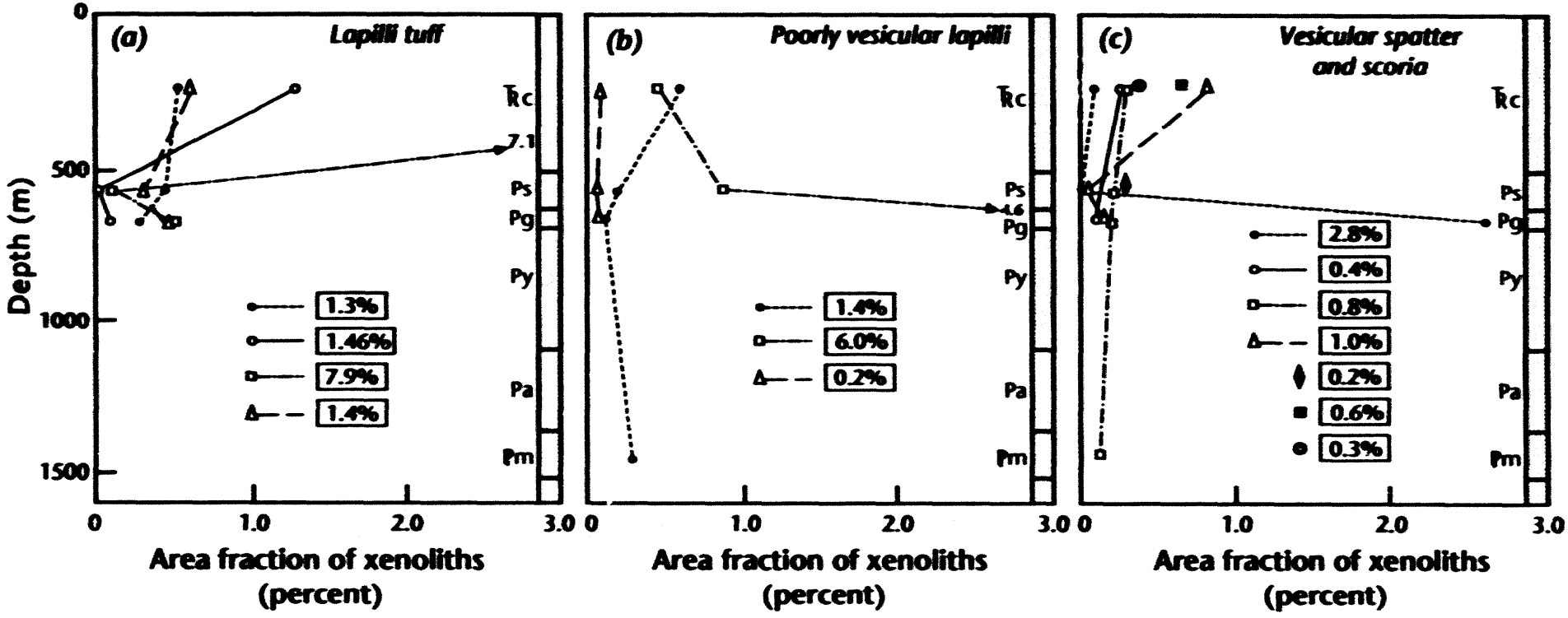
(a)
Lapilli tuff
(b)
Poorly vesicular lapilli
(c)
Vesicular spatter and scoria
Depth (m)
0
500
1000
1500
Trc
Ps
Pg
Py
Pa
Pm
7.1
4.6
1.3%
1.46%
7.9%
1.4%
1.4%
6.0%
0.2%
2.8%
0.4%
0.8%
1.0%
0.2%
0.6%
0.3%
0
1.0
2.0
3.0
Area fraction of xenoliths (percent)

Fig. 2

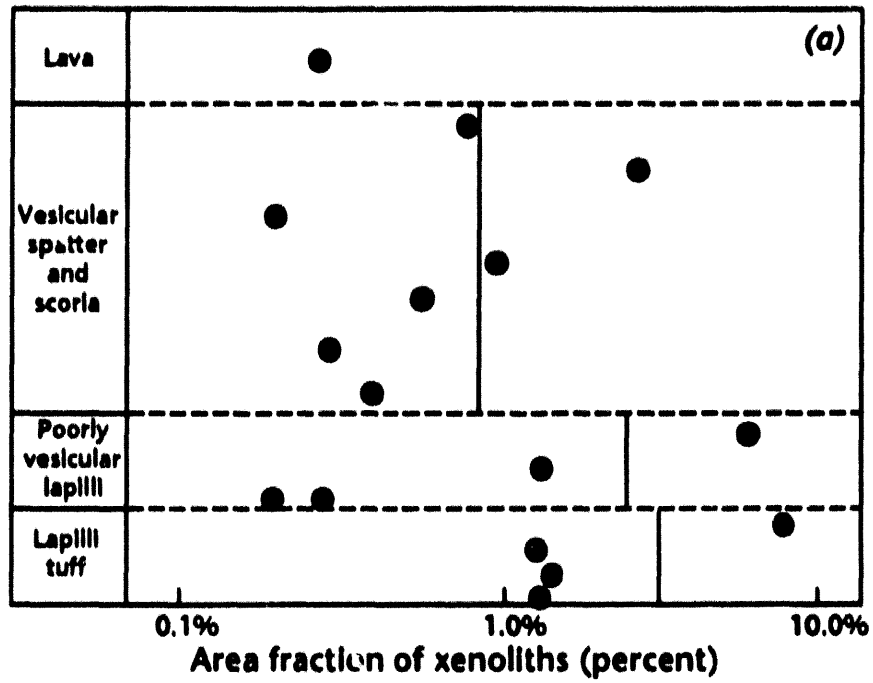
(a)
Lava
Vesicular spatter and scoria
Poorly vesicular lapilli
Lapilli tuff
0.1%
1.0%
10.0%
Area fraction of xenoliths (percent)

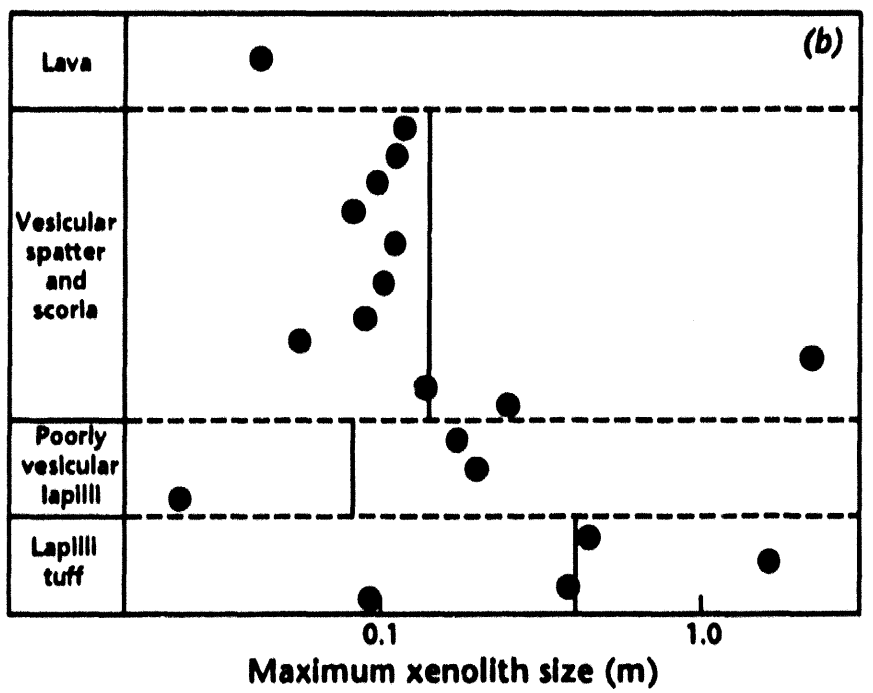
(b)
Lava
Vesicular spatter and scoria
Poorly vesicular lapilli
Lapilli tuff
0.1
1.0
Maximum xenolith size (m)

Fig. 5

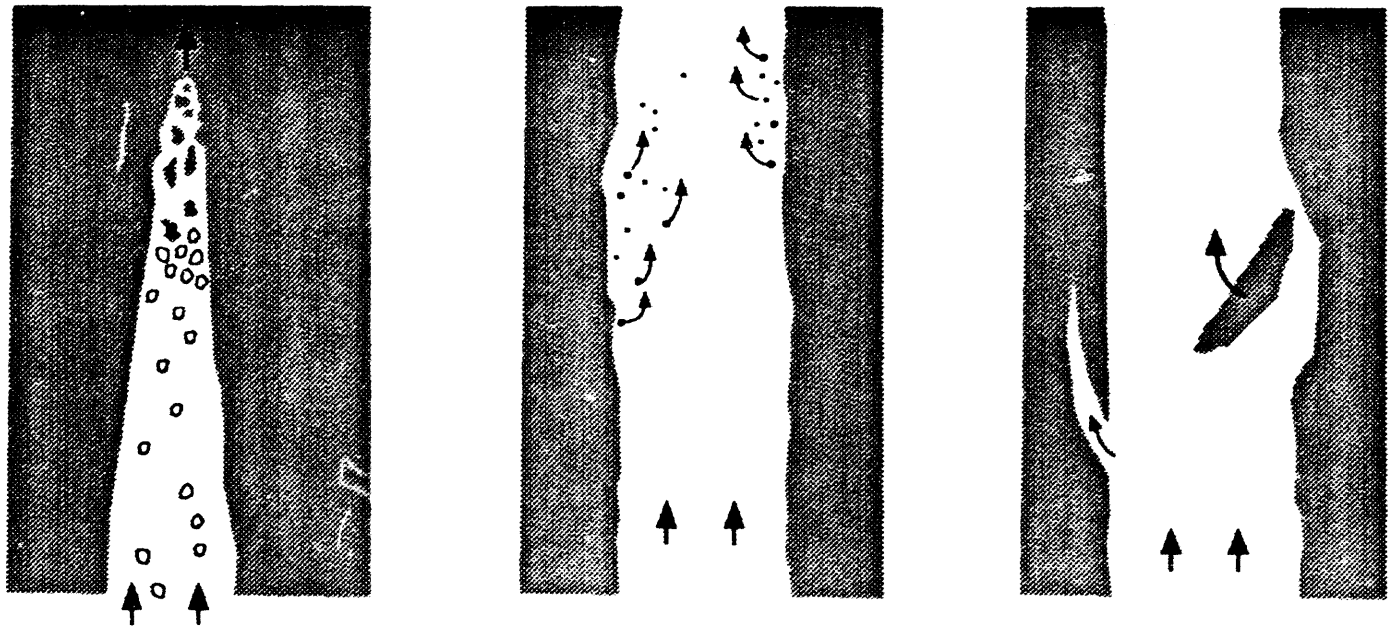
(a)
(b)
(c)

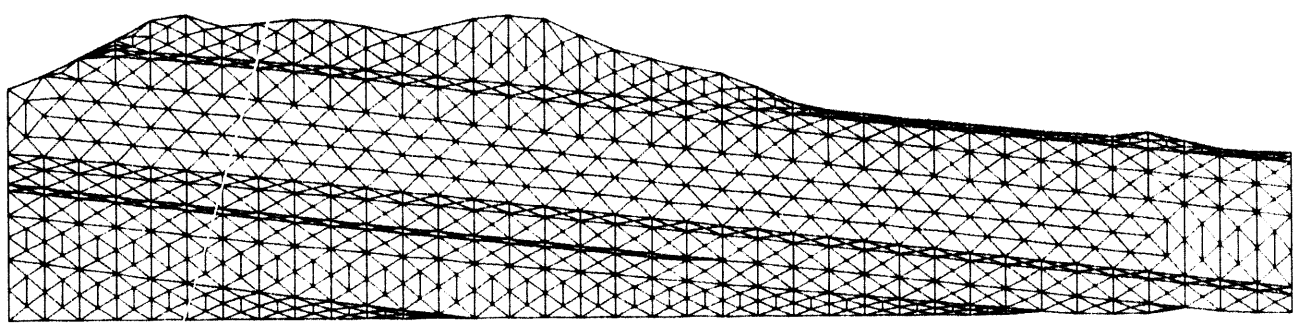

Fig. 5

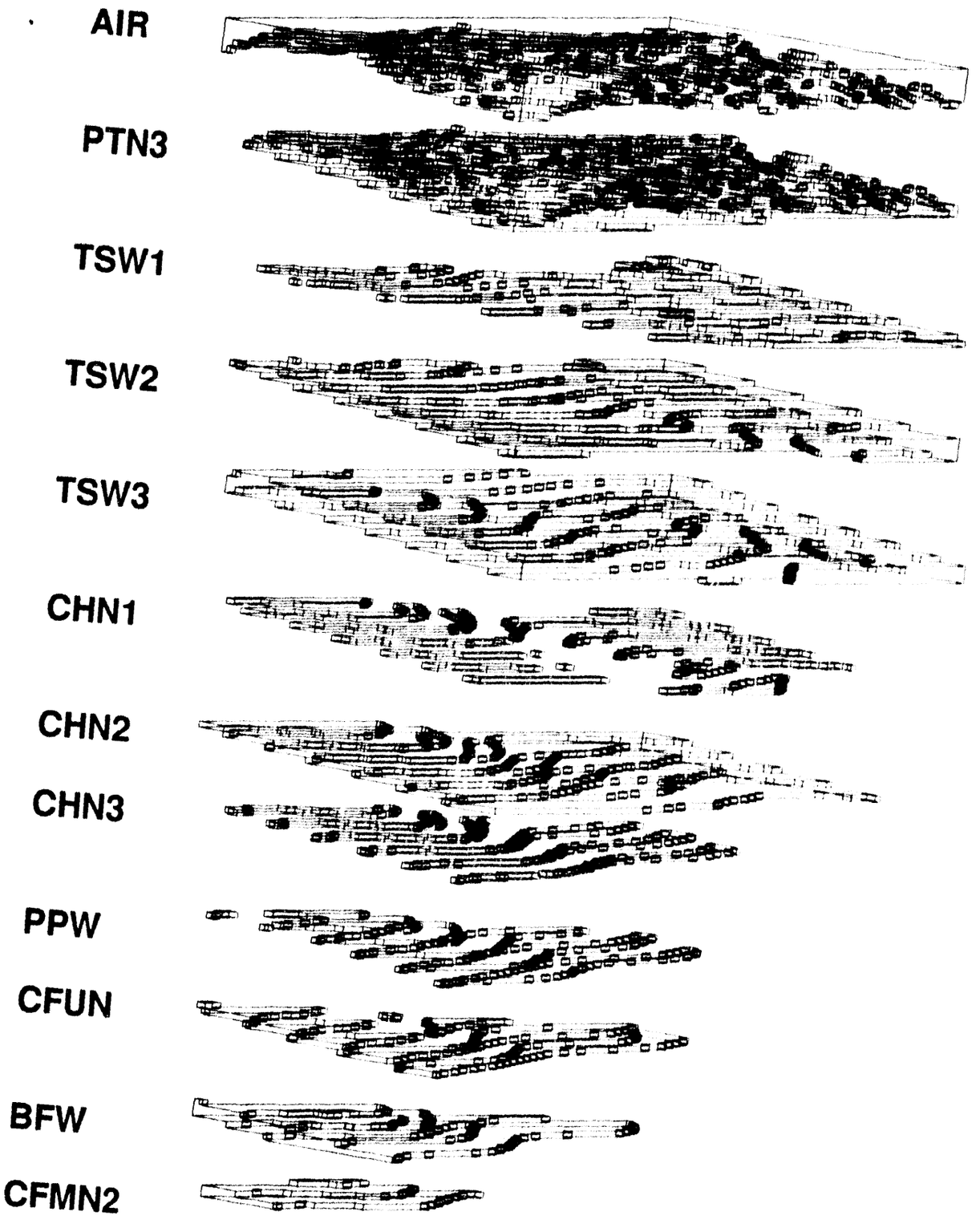

Fig. 7

DATE
FILMED
12/13/93
END